

## POSITRON ANNIHILATION SPECTROSCOPY REVEALS ENHANCEMENT OF PROTON EXCHANGE MEMBRANES BY ION IMPLANTATION

Mircea LECHINTAN<sup>1,2</sup>, Mihai STRATICIUC<sup>2\*</sup>, Nikolay DJOURELOV<sup>3</sup>, Adriana Elena BALAN<sup>4</sup>, Florin CONSTANTIN<sup>2</sup>

*Proton Exchange Membranes (PEMs) continue to be a critical focus in the development of hydrogen fuel cells, which have the potential to revolutionize the alternative energy sector. In recent years, significant progress has been made in understanding the effects of heavy ion implantation on PEMs, particularly those made from perfluorosulfonic acid (PFSA) polymers such as Fumapem® and Nafion®. In this study, we investigated the impact of platinum (Pt) ion implantation on the properties of these membranes using Positron Annihilation Spectroscopy (PAS) and direct electrical measurements.*

*Ion implantation experiments were conducted using the 3 MV Tandetron™ accelerator at IFIN-HH, with Pt<sup>1+</sup> ions at an energy of 1 MeV. Four implantation fluences were tested, ranging from  $1 \times 10^{14}$  to  $1 \times 10^{15}$  ions/cm<sup>2</sup>. The PAS analysis included Variable Energy Positron Doppler Broadening Spectroscopy (VEPDBS) and Coincidence Doppler Broadening Spectroscopy (CDBS), which provided detailed insights into the depth-dependent electronic structure modifications induced by the Pt ions.*

*Our results demonstrate a clear enhancement of ionic conductivity in all implanted samples, with the maximum conductivity observed at an implantation fluence of  $5 \times 10^{14}$  ions/cm<sup>2</sup>. This optimum fluence was found to most effectively balance the modification of proton conduction pathways and the preservation of membrane integrity. The findings underscore the potential of ion implantation as a powerful tool for tailoring the properties of PEMs to improve their performance in fuel cell applications.*

**Keywords:** fuel cell, ion implantation, polymers, positron spectroscopy, ion conductivity.

\* Corresponding author: mihai.straticiuc@cern.ch

<sup>1</sup> PhD student, SDSA, POLITEHNICA București National University for Science and Technology, București, Romania, e-mail: mircea.lechintan@nipne.ro

<sup>2</sup> Horia Hulubei National Institute for R&D in Physics and Nuclear Engineering (IFIN-HH), Magurele, Romania

<sup>3</sup> Extreme Light Infrastructure-Nuclear Physics (ELI-NP), Horia Hulubei National Institute for R&D in Physics and Nuclear Engineering (IFIN-HH), Magurele, Romania, e-mail: nikolay.djourelov@eli-np.ro

<sup>4</sup> Faculty of Physics, University of Bucharest, 3NANO-SAE Research Center, Magurele, Romania, e-mail: adriana.balan@unibuc.ro

## 1. Introduction

Proton exchange membranes (PEM) in hydrogen fuel cells are receiving special attention in the field of renewable energy. These polymers have a wide applicability in many fields of industry and research, such as: transportation, backup power systems, portable electronics, and marine and space applications [1], [2]. Fuel cells are unquestionably a "hot" research topic pursuing technological advancements and cost optimization. A membrane electrode assembly (MEA) which consists of an electrolyte, Fumasep in our case, flanked on both sides by two other layers of catalyst material, represents the heart of a fuel cell. This polymer membrane used in hydrogen fuel cells (HFC) is also referred to as PEM in scientific literature. Fumasep and Nafion membranes are among the most used as PEMs, both belonging to the perfluoro sulfonic acid (PFSA) class.

The polymer is created as a melt-processable precursor derived from  $\text{SO}_2\text{F}$  functional groups. This precursor lacks the clustered architecture but does have Teflon-like crystallinity that endures when the film is submerged in an aqueous acid solution that is sufficiently concentrated to change the sulfonyl fluoride form into the  $-\text{SO}_3\text{H}$  form [3]. There are  $\sim 40\text{\AA}$  diameter clusters of sulfonate-ended perfluoroalkyl ether groups, which are assumed to be organized as inverted micelles and arranged on a lattice, based on small-angle X-ray scattering (SAXS) experiments. Pores or channels with a diameter of  $10\text{\AA}$  connect these micelles. These  $\text{SO}_3$ -coated channels were used to explain the rejection of negative ions and intercluster ion hopping of positive charge species [4].

A deep understanding of chemical microstructure and nanoscale morphology is necessary for fine-tuning these materials in order to achieve maximum performance. Proton conductivity, water management, hydration stability at high temperatures, electro-osmotic drag, and mechanical, thermal, and oxidative stability are important characteristics that must be controlled in the logical design of these membranes [5]. Ion implantation was regarded as one of the most efficient technological methods for changing the electrical, optical, magnetic, and mechanical properties of polymers [6], [7]. Surface qualities including smoothness, adhesion, wear resistance, and chemical resistance are altered by radiation-induced effects [8], [9], [10]. Because the embedded metal atoms tend to aggregate into nanoparticles (NPs), generating metal-polymer composite materials with characteristics favorable for various applications, high-fluence metal ion implantation into polymers has drawn particular interest. Due to the significant difference in surface energy between metals and polymers, ion implantation may trigger the nucleation and development of NPs, due to the high metal concentration [11], [12].

Ion implantation in PEM has also been reported in the literature, this being performed at different fluences, with different ionic species and different energies.

By ion implantation Jung-Soo Lee *et al.* [13] obtains methanol crossover reduction in the case of Nafion PEMs when they are irradiated with protons at energies of 150 keV and fluences of up to  $10^{16}$  ions/cm<sup>2</sup>. Similar ion bombardment studies, but with Ar<sup>+</sup>, were carried out by S.A. Cho *et al.* [14] which at energies of 1.2 keV and fluences up to  $10^{17}$  ions/cm<sup>2</sup> obtained a doubling of the power density for Nafion 115 membranes (tested in HFC). This has been made possible by increasing the membrane roughness, thus enlarging the effective area of the interfaces. M.M. Nasef *et al.* [15] has a comprehensive description of how the irradiation of proton-exchange polymers can improve ionic conductivity through changes induced by radiation grafting, using different methods such as electron irradiation, gamma radiation or ion implantation.

In the present study several Fumasep 930 polymer membranes were implanted with 1 MeV Pt<sup>1+</sup> ions. We used Positron Annihilation Spectroscopy (PAS) to study the defects induced by ion implantation. PAS is a powerful analytical technique employed to study the microscopic changes induced by ion implantation [16]. By detecting the annihilation of positrons within the material, this method reveals intricate details about the membrane's structure, including alterations in pore sizes, chemical bonding, and degradation patterns. In the context of irradiated PEM membranes—critical components in fuel cells—understanding these changes is vital for optimizing performance and longevity. PAS offers invaluable insights into the conduction mechanisms of membrane protons, facilitating the development of more robust and efficient membrane technologies for energy applications.

## 2. Experimental work

### 2.1 Ion implantation

Four Fumasep (FS 930) PEM specimens were implanted with Pt ions on both sides. Implantation parameters for all samples are given in Table 1. A fifth sample was kept unirradiated as a reference sample. From the FS 930 membranes datasheet, the thickness is given in the range between 27  $\mu\text{m}$  and 31  $\mu\text{m}$ , we considered an average value of 29  $\mu\text{m}$ . The ion beam was delivered by a 3 MV Tandetron<sup>TM</sup> accelerator from Horia Hulubei National Institute for R&D in Physics and Nuclear Engineering (IFIN-HH) [17]. Ion implantation was performed through an aluminum mask shown in Fig. 1.a. with a 21×21 matrix pattern of round holes, each with a 1.6 mm diameter, summing a 50% exposure factor of the samples' total active surface. The sample holder was placed in the ion implantation chamber Fig. 2.b. at the end of the beamline. This beamline is fully equipped with horizontal and vertical -electrostatic steerers that allow uniform beam sweeping over a ~15.5 cm diameter aperture disc, as well as adequate beam monitoring. SRIM [18] simulations estimate the ion range in polymer membranes to be around 300 nm for

1 MeV Pt ions, with an average implantation depth of approximately 367 nm (Fig. 3.). The membranes were exposed to the ion beam without pretreatment since they were delivered by the manufacturer in an already activated form ( $H^+$ ). The membranes mounted in the sample holder were placed in high vacuum ( $1 \times 10^{-7}$  mbar) for two hours prior to the ion implantation in order to achieve vacuum drying.



Fig. 1.a. Ion Implantation Chamber with custom design grid sample holder installed

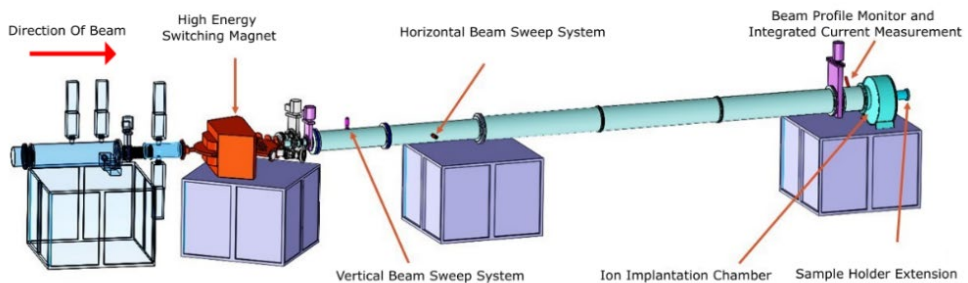


Fig. 1.b. Beam line for ion implantation at the 3 MV Tandetron™ accelerator from Horia Hulubei National Institute for R&D in Physics and Nuclear Engineering (IFIN-HH) [19]

Ion beams have the benefit of altering the surface region specifically without affecting other bulk characteristics, at room temperature [13]. One may expect that near surface changes of PEMs by heavy ion implantation will improve the ionic conductivity by increasing the surface roughness, loading with Pt in the immediate region of the catalyst layer and activating new functional groups  $-SO_3H$  by scissioning and crosslinking the fluorocarbon backbone. As a net result of these actions, it can also be considered from the perspective that the same performance

of polymer electrolyte membrane fuel cells can be obtained at a lower cost due to a diminished catalyst loading, the price of the catalyst layer being an aspect that dictates the price of a HFC system [14], [20].

Table 1

Ion implantation parameters for the PEM samples

Membrane type	Membrane thickness [μm]	Average beam current [nA/cm <sup>2</sup> ]	Irradiation time / side [h]	Ion implantation fluence / side [ions/cm <sup>2</sup> ] 2% uncertainty	Implantation energy [MeV]	Beam type
FUMASEP FS930	27-31(29)	7.3 ± 0.1	0.6	1×10 <sup>14</sup>	1	Pt <sup>1+</sup>
		7.5 ± 0.2	1.5	2.5×10 <sup>14</sup>		
		7.4 ± 0.1	3	5×10 <sup>14</sup>		
		5.5 ± 0.1	8	1×10 <sup>15</sup>		

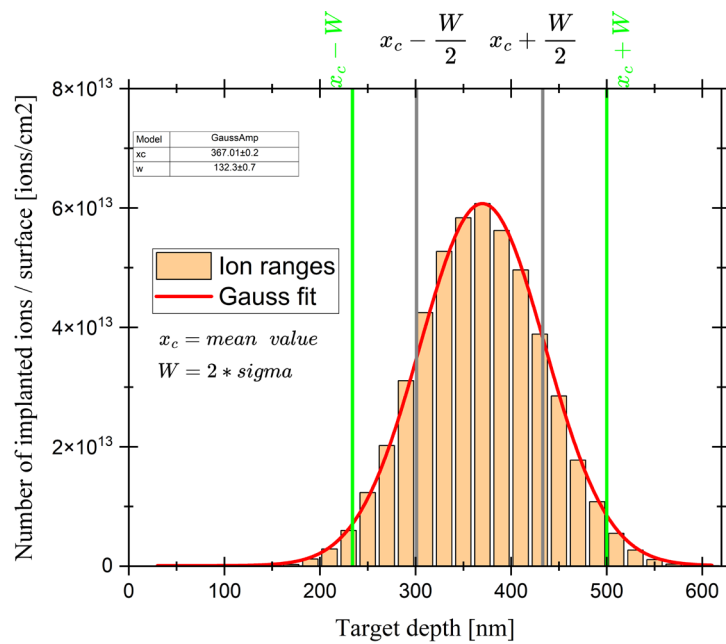


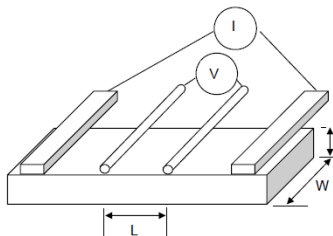
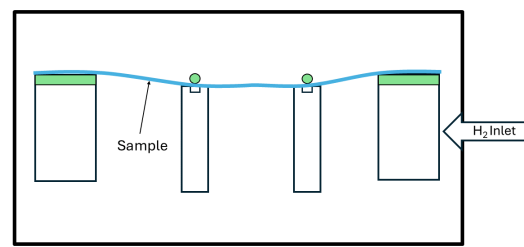
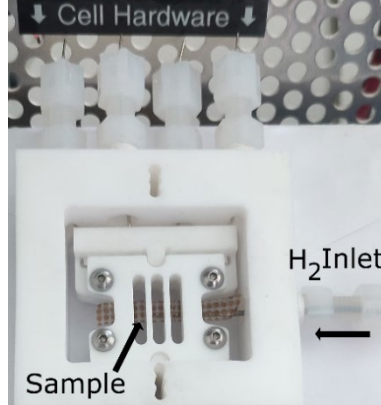
Fig. 3. Ion implantation ranges for Pt<sup>1+</sup> in Fumasep® at 1 MeV at fluence of 5×10<sup>14</sup> ions/cm<sup>2</sup>.

## 2.2 Electrical characterization of the PEM

The ionic conductivity of PEMs is a critical parameter in fuel cell applications, as it directly influences the efficiency of proton (H<sup>+</sup>) transport from

the anode to the cathode. High ionic conductivity is essential for minimizing internal resistance, thereby enhancing the overall efficiency and power output of the fuel cell. To achieve this, maintaining optimal hydration levels within the membrane is crucial, as it supports consistent proton conductivity across a range of temperatures and environmental conditions.

To assess the impact of Pt ion implantation on the ionic conductivity of the membranes, a series of measurements were conducted on all four implanted samples, along with a reference sample. The measurements were carried out using a conductivity test cell manufactured by Bekktech [21]. In this setup, each sample, with a shape of a  $5\text{ mm} \times 40\text{ mm}$  strip, was placed in contact with four platinum electrodes. A bias voltage was applied to the two interior electrodes, and the resulting current was measured using the two exterior mesh electrodes while the sample was exposed to hydrogen gas. The gas, maintained at atmospheric pressure and heated to  $80^\circ\text{C}$ , was passed through a saturator to achieve different relative humidities. This setup allowed for the precise evaluation of the ionic conductivity under controlled conditions. A schematic of the test setup is presented in Fig. 4, and a photograph of the test cell is shown in Fig. 5. The conductivity measurement technique is a standard one, it being presented in the reference [22].

 	
<p>Fig. 4. Four-point measurement with platinum electrodes (see text for details) [22]</p>	<p>Fig. 5. The disassembled test cell with the implanted sample positioned in contact with the electrodes</p>

### 2.3 PAS analysis of the ion implanted PEM

We employed in our work a version of the PAS analysis named Coincidence Doppler Broadening Spectroscopy (CDBS). This analysis provides a complementary understanding of the change in proton conduction mechanisms of the Fumasep membranes. CDBS technique analyzes the electronic environment around positron annihilation sites in a material. This method provides information on the chemical composition, electron density, and defects within the material [23], [24]. The analysis was carried out with the help of an intense beam of slow positrons ( $5 \times 10^6$  positrons/s) obtained by solid neon moderation [25]. Slow positron laboratory beam from Extreme Light Infrastructure - Nuclear Physics (ELI-NP) offers the possibility of performing analyzes with monoenergetic positrons in the energy range 0.5 - 30 keV. The positrons are obtained from  $^{22}\text{Na}$  radioactive sources (activity 50 mCi, half-life  $\sim 2.6\text{y}$ ). All four ion implanted samples, and the reference one was analyzed. The Doppler shifted annihilation gamma photons were detected by two HPGe detectors positioned in head-to-head geometry, with an energy resolution of approximately 1.3 keV@511 keV. Before performing the coincidence analysis, a series of measurements was done in non-coincidence mode with Variable Energy Positron Doppler Broadening Spectroscopy (VEPDBS) [26] to depth profiling the defect density induced by the Pt ions implantation in the Fumasep sample. The energy of the positron beam was changed in steps of 0.5 keV for the range 0.5-6 keV, then in steps of 1 keV until the maximum energy of 25 keV. CDBS measurements were performed at 5.5 keV positron beam energy. In coincidence mode, the background is considerably reduced approximately 80 times, at the expense of much longer acquisition time which can be up to 50 times higher for the same number of recorded events.

## 3. Results and discussion

### 3.1 Ion conductivity

We measured the ionic conductivity of Fumasep membranes implanted with Pt ions by using the setup presented in Fig. 4 and Fig. 5 described in the previous section. The measurement was performed at different values of the relative humidity of the  $\text{H}_2$  gas injected in the test cell. The obtained values are presented in Fig. 6.

These results indicate a clear relationship between the implantation fluence and the membrane's proton conduction capabilities. As expected, the ionic conductivity increases with relative humidity for all samples, reflecting the enhanced proton transport due to better hydration of the membrane.

Among the different fluences tested, the sample implanted with  $5 \times 10^{14}$  ions/ $\text{cm}^2$  exhibited the highest ionic conductivity across the majority of the

humidity range. This suggests that this specific implantation fluence optimally modifies the microstructure of the Fumasep membrane, enhancing the connectivity of proton conduction pathways. The introduction of Pt ions at this fluence likely facilitates an ideal distribution of functional groups and hydration channels, which are crucial for efficient proton transport. This mechanism is suggested by ref. [27].

However, a further increase in the implantation fluence to  $1 \times 10^{15}$  ions/cm<sup>2</sup> resulted in a slight reduction of the membrane conductivity. This decline suggests that excessive ion implantation may lead to structural damage or the agglomeration of Pt particles, which can disrupt the delicate balance of proton conduction pathways within the membrane [28], [29]. The results of the present measurements show that ion implantation can significantly enhance the ionic conductivity of Fumasep membranes, the value of the fluence must be carefully optimized to maximize conductivity.

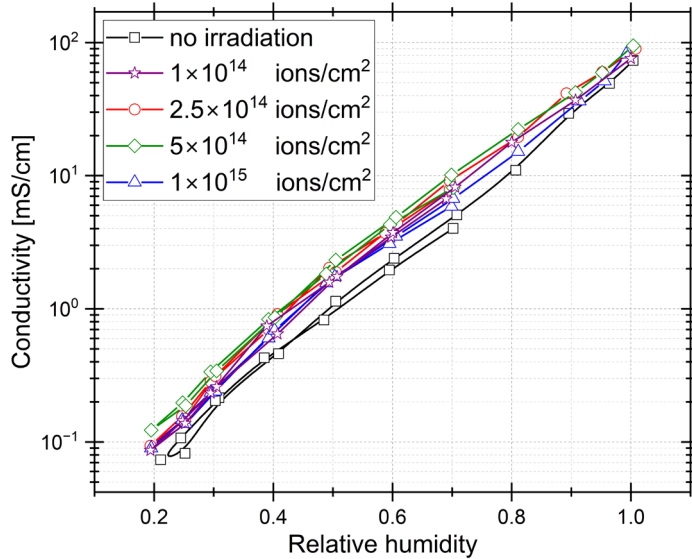


Fig. 6. Ionic conductivity of PEM before (squares) and after implantation (all other symbols) with Pt ions. All samples measured in H<sub>2</sub> atmosphere at 80°C.

### 3.2 PAS measurements

Before conducting the CDBS analysis, it was important to perform VEPDBS ranging from 0.5 to 30 keV as discussed in section 2.3. By varying the positron energy, we were able to selectively explore different depths within the membrane. This preliminary step was necessary to probe the specific implanted

regions of the Fumasep membrane, where Pt ions were stopped. By varying the positron energy, we were able to selectively explore different depths within the membrane, allowing us to identify the regions most affected by implantation. The VEPDBS analysis focused on measuring the  $W$ -parameter (associated with high-momentum electron annihilation) to detect changes in the local electronic environment in the regions most affected by Pt implantation. Understanding the depth profile and the extent of the change in  $W$ -values was essential for accurately interpreting the subsequent CDBS data. It ensured that the analysis focused on the depth where the maximum of the ion implantation occurs. VEPDBS results are shown in Fig. 7. for the  $W$ -parameter.

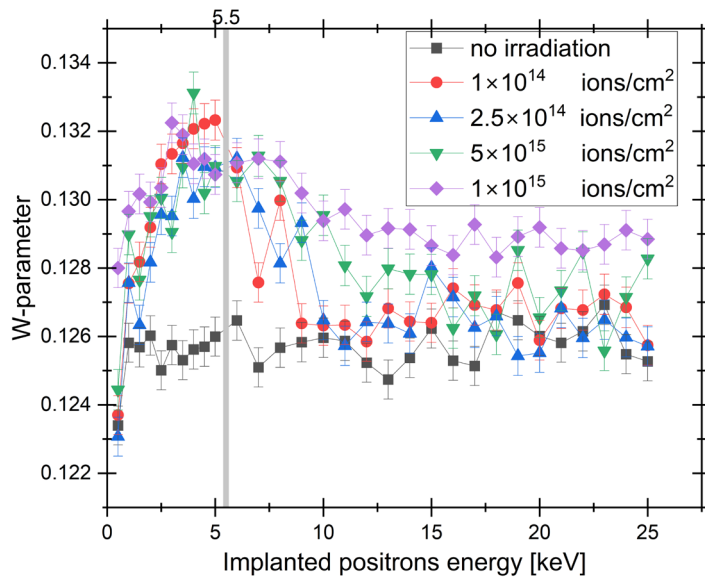


Fig. 7. Depth profiling with VEPDBS,  $W$  value represents the fraction of annihilation events with high momentum electrons.

VEPDBS analysis revealed significant changes at a positron energy of 5.5 keV in Fumasep samples implanted with varying fluences of Pt ions. This marked change in the  $W$ -parameter, particularly in samples with higher implantation fluences, indicates a strong interaction between positrons and the defects induced by implanted Pt ions at this specific depth. The results suggest that the modifications in the local electronic environment are directly due to the presence of platinum within the membrane, highlighting the effectiveness of this technique in probing the implanted region.

Modeling of the positron paths in the Fumasep sample is important for accurately interpreting depth profiling results, as it provides a predictive model of how positrons interact with the material at various energies. The modeling thus

ensures that the observed changes in the  $W$ -parameter are correctly attributed to specific depths, validating the analysis and ensuring that the experimental findings are directly linked to the modifications introduced by ion implantation. The modeled theoretical data of the positron trajectory profile in the sample are presented in Fig. 8.

The positron implantation profile was taken as:

$$P(z, E) = 2z/z_0^2 \exp(-(z/z_0)^2), \quad (1)$$

where  $E$  is the incident  $e^+$  energy in keV,  $z$  in nm is the depth,

$$z_0 = 2 z_m / \sqrt{\pi}, \quad (2)$$

where the mean penetration depth is determined by  $z_m$ , the density  $\rho$  is in  $\text{g/cm}^3$  [30].

$$z_m = (36/\rho)E^{1.62}. \quad (3)$$

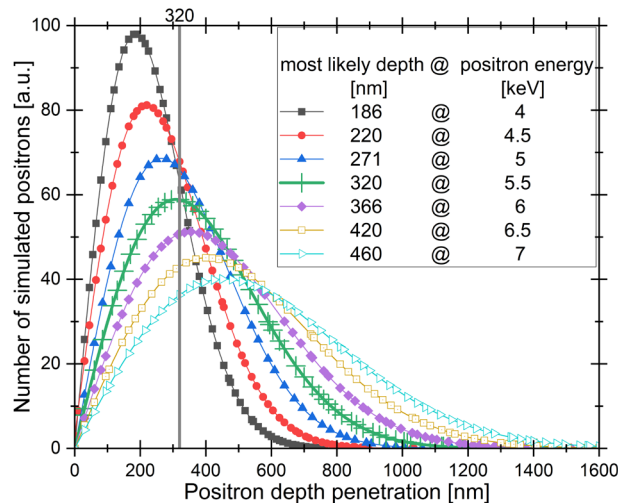


Fig. 8. Positron profile implantation

The positron path simulation, which models the penetration depth of positrons at various energies, indicates that at 5.5 keV, positrons predominantly probe to a depth of approximately 320 nm within the Fumasep membrane. This depth corresponds closely with the region where significant changes in the  $W$ -parameter were observed, suggesting that positrons at this energy are effectively interacting with the defects induced by implanted Pt ions. Therefore the agreement confirms that the positrons are probing the specific depths influenced by the ion implantation, validating the depth sensitivity of the profiling technique, which is

further reinforced by the data presented in section 2.1, where SRIM simulation of Pt ion ranges in Fumasep (Fig. 2.) revealed that the ions are primarily implanted at a mean depth ( $x_c$ ) of approximately 367 nm, with a distribution spanning from 230 nm to 500 nm within 2 sigma ( $W$ ), containing slightly more than 95% of the implanted ions. This depth range closely matches the region probed by positrons at 5.5 keV, confirming that the observed electronic modifications are directly linked to the presence of implanted Pt ions within these specific depths. Hence, the energy of 5.5 keV was chosen to perform the CDBS measurements and the results are presented in Fig. 9.

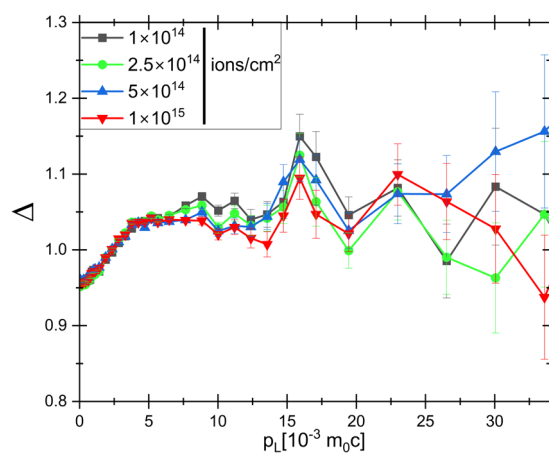


Fig. 9. CDBS positron beam analysis, with  $\Delta$  as the relative value compared to the reference sample FS 930 and  $p_L$  represents the longitudinal component of the electron momentum in the direction of the positron annihilation gamma rays.

The CDBS analysis of Fumasep membranes implanted with varying fluences of Pt ions reveals significant insights into the electronic structure modifications induced by ion implantation. The delta function ( $\Delta$ ) in the CDBS analysis represents the ratio of high-momentum to low-momentum electron interactions, providing insight into the presence of high-momentum core electrons. The data presented in the CDBS graph are relative to the non-implanted sample, allowing for a direct comparison of how Pt ion implantation at different fluences alters the electronic structure of the Fumasep membrane. The CDBS data indicates an increasing trend in the delta function values as the implantation fluence increases, particularly in the high-momentum region ( $15-30 \times 10^{-3} m_0 c$ ). This rise in the delta function suggests enhanced interactions between positrons and high-momentum core electrons, likely originating from the implanted Pt atoms.

Interestingly, the sample implanted at  $5 \times 10^{14}$  ions/cm<sup>2</sup> shows a distinct peak in the delta function, indicating an optimal incorporation of platinum that

maximizes the interaction with core electrons. This correlates strongly with the highest observed ionic conductivity for this sample, suggesting that this implantation fluence achieves the best balance between modifying the electronic structure and enhancing proton conduction pathways.

In contrast, at the highest fluence of  $1 \times 10^{15}$  ions/cm<sup>2</sup>, the CDBS profile becomes less favorable, with a less pronounced delta function peak. This change corresponds with a decrease in ionic conductivity, likely due to excessive platinum accumulation, which may introduce defects or disrupt the continuity of proton conduction channels.

## 6. Conclusions

The systematic investigation of Pt ion implantation effects on the ionic conductivity and electronic structure of Fumasep membranes is described, with a focus on understanding how varying implantation fluences impact these properties. Our findings demonstrate that the optimal fluence for enhancing ionic conductivity is  $5 \times 10^{14}$  ions/cm<sup>2</sup>, where the proton conduction pathways are most effectively modified. This specific implantation fluence appears to strike a balance that optimizes the distribution of functional groups and hydration channels, thereby facilitating efficient proton transport across the membrane.

Depth profiling analysis using Variable Energy Positron Doppler Broadening Spectroscopy (VEPDBS) revealed significant changes in the *W*-parameter at a positron energy of 5.5 keV, correlating with the depths where Pt ions are primarily implanted. This observation was further supported by positron path simulations, which confirmed that positrons at this energy predominantly interact with the implanted regions, validating the depth sensitivity of the profiling technique.

The subsequent Coincidence Doppler Broadening Spectroscopy (CDBS) analysis provided deeper insights into the electronic structure modifications induced by Pt implantation. The CDBS data indicated an increasing trend in high-momentum electron interactions with increasing fluence, with a distinct peak observed at  $5 \times 10^{14}$  ions/cm<sup>2</sup> aligning with the highest ionic conductivity. Conversely, at the highest fluence of  $1 \times 10^{15}$  ions/cm<sup>2</sup> the CDBS profile suggested a less favorable modification of the electronic structure, corresponding to a decline in conductivity, likely due to platinum agglomeration or structural disruptions.

In conclusion, Pt ion implantation at carefully controlled fluences can significantly enhance the performance of Fumasep membranes by optimizing proton conduction pathways and electronic structure. However, excessive implantation can lead to detrimental effects, underscoring the importance of fluence optimization in achieving the desired balance between conductivity enhancement and structural integrity. These findings contribute to the broader understanding of

ion implantation as a powerful tool for tailoring the properties of proton exchange membranes in fuel cell applications.

## R E F E R E N C E S

- [1] *N. L. Garland, D. C. Papageorgopoulos, and J. M. Stanford*, “Hydrogen and Fuel Cell Technology: Progress, Challenges, and Future Directions,” *Energy Procedia*, vol. 28, pp. 2–11, 2012, doi: 10.1016/j.egypro.2012.08.034.
- [2] *H. Montazerinejad, E. Fakhimi, S. Ghandehariun, and P. Ahmadi*, “Advanced exergy analysis of a PEM fuel cell with hydrogen energy storage integrated with organic Rankine cycle for electricity generation,” *Sustainable Energy Technologies and Assessments*, vol. 51, p. 101885, Jun. 2022, doi: 10.1016/j.seta.2021.101885.
- [3] *W. G. Grot*, “Nafion® membrane and its applications,” in *Electrochemistry in Industry: New Directions*, Springer, 1982, pp. 73–87.
- [4] *T. D. Gierke, G. E. Munn, and F. C. Wilson*, “The morphology in nafion perfluorinated membrane products, as determined by wide- and small-angle x-ray studies,” *J. Polym. Sci. Polym. Phys. Ed.*, vol. 19, no. 11, pp. 1687–1704, Nov. 1981, doi: 10.1002/pol.1981.180191103.
- [5] *K. A. Mauritz and R. B. Moore*, “State of Understanding of Nafion,” *Chem. Rev.*, vol. 104, no. 10, pp. 4535–4586, Oct. 2004, doi: 10.1021/cr0207123.
- [6] *F. Di Benedetto et al.*, “Strain gauge properties of  $Pd^{+}$ -ion-implanted polymer,” *Nanomaterials and Nanotechnology*, vol. 10, p. 184798042094797, Jan. 2020, doi: 10.1177/1847980420947975.
- [7] *V. Popok*, “Compositional and structural alterations of polymers under low-to-medium energy ion implantation,” 2005, pp. 147–193.
- [8] *R. J. Rodríguez, J. A. García, R. Sánchez, A. Pérez, B. Garrido, and J. Morante*, “Modification of surface mechanical properties of polycarbonate by ion implantation,” *Surface and Coatings Technology*, vol. 158–159, pp. 636–642, Sep. 2002, doi: 10.1016/S0257-8972(02)00322-5.
- [9] *E. H. Lee, M. B. Lewis, P. J. Blau, and L. K. Mansur*, “Improved surface properties of polymer materials by multiple ion beam treatment,” *J. Mater. Res.*, vol. 6, no. 3, pp. 610–628, Mar. 1991, doi: 10.1557/JMR.1991.0610.
- [10] *F. Ruffino, V. Torrisi, G. Marletta, and M. G. Grimaldi*, “Effects of the embedding kinetics on the surface nano-morphology of nano-grained Au and Ag films on PS and PMMA layers annealed above the glass transition temperature,” *Appl. Phys. A*, vol. 107, no. 3, pp. 669–683, Jun. 2012, doi: 10.1007/s00339-012-6842-5.
- [11] *Y. Wang, L. B. Bridwell, and R. E. Giedd*, “Composite conduction in ion-implanted polymers,” *Journal of Applied Physics*, vol. 73, no. 1, pp. 474–476, Jan. 1993, doi: 10.1063/1.353824.
- [12] *D. Fink and V. Hnatowicz*, “Transport Processes in Low-Energy Ion-Irradiated Polymers,” in *Transport Processes in Ion-Irradiated Polymers*, vol. 65, in *Springer Series in Materials Science*, vol. 65. , Berlin, Heidelberg: Springer Berlin Heidelberg, 2004, pp. 47–91. doi: 10.1007/978-3-662-10608-2\_2.
- [13] *J.-S. Lee, I.-T. Hwang, C.-H. Jung, and J.-H. Choi*, “Surface modification of Nafion membranes by ion implantation to reduce methanol crossover in direct methanol fuel cells,” *RSC Adv.*, vol. 6, no. 67, pp. 62467–62470, 2016, doi: 10.1039/C6RA12756H.
- [14] *S. A. Cho et al.*, “Surface modified Nafion® membrane by ion beam bombardment for fuel cell applications,” *Journal of Power Sources*, vol. 155, no. 2, pp. 286–290, Apr. 2006, doi: 10.1016/j.jpowsour.2005.05.040.

- [15] *M. Nasef*, “Preparation and applications of ion exchange membranes by radiation-induced graft copolymerization of polar monomers onto non-polar films,” *Progress in Polymer Science*, vol. 29, no. 6, pp. 499–561, Jun. 2004, doi: 10.1016/j.progpolymsci.2004.01.003.
- [16] Slugen and V Institute for Energy and Transport (Joint Research Centre), What kind of information we can obtain from positron annihilation spectroscopy?, vol. 22468. 2006.
- [17] I. Burducea *et al.*, “A new ion beam facility based on a 3 MV Tandetron™ at IFIN-HH, Romania,” *Nuclear Instruments and Methods in Physics Research Section B: Beam Interactions with Materials and Atoms*, vol. 359, pp. 12–19, Sep. 2015, doi: 10.1016/j.nimb.2015.07.011.
- [18] J. F. Ziegler, M. D. Ziegler, and J. P. Biersack, “SRIM – The stopping and range of ions in matter (2010),” *Nuclear Instruments and Methods in Physics Research Section B: Beam Interactions with Materials and Atoms*, vol. 268, no. 11–12, pp. 1818–1823, Jun. 2010, doi: 10.1016/j.nimb.2010.02.091.
- [19] R.-F. Andrei and I. Decebal, “Ion Implantation Modular Setup Upgrade for the 3 Mv Tandetron at IFIN-HH,” *Romanian Journal of Physics*, vol. 67, p. 302, Jan. 2022.
- [20] M. Prasanna, E. A. Cho, H.-J. Kim, T.-H. Lim, I.-H. Oh, and S.-A. Hong, “Effects of platinum loading on performance of proton-exchange membrane fuel cells using surface-modified Nafion® membranes,” *Journal of Power Sources*, vol. 160, no. 1, pp. 90–96, Sep. 2006, doi: 10.1016/j.jpowsour.2006.01.071.
- [21] “<https://www.alvatek.co.uk/>.”
- [22] Adriana Elena Andronie, “Preparation and Characterization of New Materials with Proton Conductivity for Applications in Fuel Cells,” Ph.D. Thesis, University of Bucharest, The faculty of physics, 2011.
- [23] A. Biganeh, O. Kakuee, H. Rafi-Kheiri, M. Lamehi-Rachti, N. Sheikh, and E. Yahaghi, “Positron Annihilation Lifetime and Doppler Broadening Spectroscopy of polymers,” *Radiation Physics and Chemistry*, vol. 166, p. 108461, Jan. 2020, doi: 10.1016/j.radphyschem.2019.108461.
- [24] R. A. Hakvoort, *Applications of positron depth profiling*. 1993.
- [25] N. Djourelov, D. Dinescu, and V. Leca, “An overview of the design of ELIPS—A new slow positron beam line,” *Nuclear Instruments and Methods in Physics Research Section A: Accelerators, Spectrometers, Detectors and Associated Equipment*, vol. 934, pp. 19–25, Aug. 2019, doi: 10.1016/j.nima.2019.04.032.
- [26] G. Dlubek, F. Börner, R. Buchhold, K. Sahre, R. Krause-Rehberg, and K.-J. Eichhorn, “Damage-depth profiling of ion-irradiated polyimide films with a variable-energy positron beam,” *J. Polym. Sci. B Polym. Phys.*, vol. 38, no. 23, pp. 3062–3069, Dec. 2000, doi: 10.1002/1099-0488(20001201)38:23<3062::AID-POLB80>3.0.CO;2-I.
- [27] S. J. Peighambarioust, S. Rowshanzamir, and M. Amjadi, “Review of the proton exchange membranes for fuel cell applications,” *International Journal of Hydrogen Energy*, vol. 35, no. 17, pp. 9349–9384, Sep. 2010, doi: 10.1016/j.ijhydene.2010.05.017.
- [28] N. W. DeLuca and Y. A. Elabd, “Polymer electrolyte membranes for the direct methanol fuel cell: A review,” *J Polym Sci B Polym Phys*, vol. 44, no. 16, pp. 2201–2225, Aug. 2006, doi: 10.1002/polb.20861.
- [29] W. H. J. Hogarth, J. C. Diniz Da Costa, and G. Q. (Max) Lu, “Solid acid membranes for high temperature ( $\geq 140^\circ \text{C}$ ) proton exchange membrane fuel cells,” *Journal of Power Sources*, vol. 142, no. 1–2, pp. 223–237, Mar. 2005, doi: 10.1016/j.jpowsour.2004.11.020.
- [30] A. Vehanen, K. Saarinen, P. Hautojärvi, and H. Huomo, “Profiling multilayer structures with monoenergetic positrons,” *Phys. Rev. B*, vol. 35, no. 10, pp. 4606–4610, Apr. 1987, doi: 10.1103/PhysRevB.35.4606.